



**AALBORG UNIVERSITY**  
DENMARK

**Aalborg Universitet**

## **Grid synchronization for distributed generations**

Oshnoei, Arman; Peyghami, Saeed; Mokhtari, Hossein; Blaabjerg, Frede

*Published in:*  
Encyclopedia of Sustainable Technologies

*DOI (link to publication from Publisher):*  
[10.1016/B978-0-323-90386-8.00079-6](https://doi.org/10.1016/B978-0-323-90386-8.00079-6)

*Publication date:*  
2023

*Document Version*  
Accepted author manuscript, peer reviewed version

[Link to publication from Aalborg University](#)

*Citation for published version (APA):*  
Oshnoei, A., Peyghami, S., Mokhtari, H., & Blaabjerg, F. (2023). Grid synchronization for distributed generations. In *Encyclopedia of Sustainable Technologies* (2 ed., pp. 1-21). Elsevier. <https://doi.org/10.1016/B978-0-323-90386-8.00079-6>

### **General rights**

Copyright and moral rights for the publications made accessible in the public portal are retained by the authors and/or other copyright owners and it is a condition of accessing publications that users recognise and abide by the legal requirements associated with these rights.

- Users may download and print one copy of any publication from the public portal for the purpose of private study or research.
- You may not further distribute the material or use it for any profit-making activity or commercial gain
- You may freely distribute the URL identifying the publication in the public portal -

### **Take down policy**

If you believe that this document breaches copyright please contact us at [vbn@aub.aau.dk](mailto:vbn@aub.aau.dk) providing details, and we will remove access to the work immediately and investigate your claim.

# Grid synchronization for distributed generations

Arman Oshnoei<sup>1</sup>, Saeed Peyghami<sup>1</sup>, Hossein Mokhtari<sup>2</sup>, Frede Blaabjerg<sup>1</sup>

<sup>1</sup>Department of Energy Technology, Aalborg University, Aalborg, Denmark

(*aros@energy.aau.dk*, *sap@energy.aau.dk*, *fbl@energy.aau.dk*)

<sup>2</sup>Department of Electrical Engineering, Sharif University of Technology, Tehran, Iran  
(*mokhtari@sharif.edu*)

**Abstract:** Distributed Generators (DGs) like photovoltaic arrays, wind turbines, and fuel cell modules, as well as Distributed Storage (DS) units introduce some advantages to the power systems and make it more reliable, flexible, and controllable in comparison with the conventional power systems. Grid interface of the different DGs is dependent on the prime energy resources, and it can be a synchronous/asynchronous generator, and a power electronic converter to control the power. However, depending on the interaction with the grid, power electronic interfaced DGs can be categorized into two main groups: grid-following (GFL) inverters and grid-forming (GFM) inverters. Both type of interfaces needs to be synchronized with the grid or micro-grid, and hence, a precise synchronization algorithm is required to estimate the phase angle and frequency of the voltage at the coupling point. Unlike synchronous generators, in power electronic interfaced DGs, synchronization signals are not only utilized during start-up, but also employed by control system to form the sinusoidal voltage waveforms. Since the control system relies on the synchronization signals, any delay and inaccuracy in estimation algorithms may make an interaction between the DG/DS and the utility grid. Therefore, the synchronization is a crucial issue in power electronic interfaced DGs to have a stable and reliable operation. In this chapter, the GFL and GFM modes for power electronic interfaced DGs are categorized from a control system standpoint, and then their grid-synchronization principles are reviewed.

**Keywords:** Distributed Generation, Grid Connection, Grid-following (GFL) inverter, Grid-forming (GFL) inverter, Phase-locked loop, Renewable resources, Voltage-source converters.

## KEY POINTS/OBJECTIVES

The main contributions of this chapter are summarized as follows:

- The GFL and GFM modes for power electronic interfaced DGs are outlined from the control system point of view.
- A comparison of GFL and GFM inverters, highlighting their salient features is provided.
- The general grid-synchronization principles for GFL and GFM modes are reviewed.

## Table of Contents

|            |   |           |
|------------|---|-----------|
| <b>1.1</b> | <b>Introduction</b>   | <b>3</b>  |
| 1.1.1      | Functionality of the Synchronization in Power Systems                     | 3         |
| 1.1.2      | Grid Synchronization Methods  | 4         |
| <b>1.2</b> | <b>Classification of Distributed Generations</b>                          | <b>5</b>  |
| 1.2.1      | Grid Following DGs  | 6         |
| 1.2.2      | Grid Forming DGs  | 9         |
| 1.2.3      | Performance comparison between GFL and GFM inverters                      | 11        |
| <b>1.3</b> | <b>Grid-synchronization methods– GFL inverters</b>                        | <b>12</b> |
| 1.3.1      | Single Phase – PLL  | 12        |
| 1.3.2      | Basic Structure of a PLL  | 12        |
| 1.3.3      | OSG Based PLL   | 13        |
| 1.3.4      | DC Component Rejection  | 16        |
| 1.3.5      | Three Phase – PLL   | 18        |
| 1.3.6      | Basic Structure of PLL  | 18        |
| 1.3.7      | Synchronous Reference Frame PLL for Unbalanced and Distorted Grid Voltage | 18        |
| 1.3.8      | Stationary Reference Frame Double SOGI PLL for Unbalanced Grid Voltage    | 19        |
| 1.3.9      | Synchronization for Power Quality Improvement                             | 21        |
| <b>1.4</b> | <b>Grid-synchronization methods– GFM inverters</b>                        | <b>23</b> |
| 1.4.1      | Droop control   | 23        |
| 1.4.2      | Droop control with LPFs   | 24        |
| 1.4.3      | SG-based droop control  | 25        |
| <b>1.5</b> | <b>Summary</b>  | <b>27</b> |
|            | <b>References</b>   | <b>29</b> |

## 1.1 Introduction

In an ac power grid, the frequency and phase angle of the voltage at the coupling point of the utility grid is an essential piece of information used in operation, control, and protection. Conventionally, synchronous generators need to be synchronized with the grid to supply the power into the grid. The phase angle, frequency and phase sequence of the output voltage of the synchronous generator have to be close enough to that of the voltage at the coupling point (Chapman 2005). Otherwise, connecting the generator into the grid may damage the generator windings and/or turbo-generator shaft. After synchronization, all synchronous generators connected to the utility grid, can work with a unique synchronous frequency (Kundur et al. 1994). There are two type of synchronous generators from the primary control stand point, droop controlled generators, and fixed PQ controlled generators.

Droop controlled generators will be synchronized together through the speed droop control of the governor system, and the frequency of the utility grid will be imposed by these generators. However, fixed PQ generators only supply the scheduled active ( $P$ ) and reactive ( $Q$ ) power into the grid with the frequency imposed by the utility grid, and the governor control system in these generators employs a Proportional-Integrator (PI) regulator to control the generator speed to be equal to the grid frequency (Woodward Manual 2004). Therefore, in conventional power systems, after synchronizing with the utility grid, the synchronous generators will still synchronously operate by means of the governor system.

Furthermore, synchronous generators naturally generate a three-phase sinusoidal voltage at the terminals with a frequency dictated by the speed of turbine. Therefore, a mechanical system determines the frequency of the generated voltage. Balanced three-phase voltages are also generated by the distributed windings on the stator of the generator. Hence, the frequency is imposed by the governor system, and the balanced three phase voltage is induced in the distributed winding by the air gap flux (Fitzgerald et al. 1990).

However, most of the Distributed Generators (DGs) and Distributed Storage (DS) systems including solar, wind, battery and etc., interface with the grid by utilizing a power electronic converter (inverter). Therefore, there are no mechanical or physical mechanisms to generate the sinusoidal voltages. However, the ac voltages are generated by turning on/off of the power electronic switches such as IGBTs, MOSFETs, etc. Moreover, like synchronous generators, connection of the power electronic converters into the grid should be performed at the same voltage parameters of the coupling point. Otherwise, the converter may be damaged due to the inrush current. More functionalities of the synchronization system are explained in the following.

### 1.1.1 Functionality of the Synchronization in Power Systems

As already mentioned, in converter-based DGs, the sinusoidal voltage waveforms are formed by turning on/off of the power electronic switches with a high frequency – e.g., 2 kHz up to 200 kHz – based on the converter rating. A sinusoidal carrier signal is used to generate the output voltage by the converter. The carrier signal should be in phase with the grid voltage in order to have a proper operation of the converter. Hence, a synchronization system should accurately estimate the grid voltage phase angle. Any delay caused by the synchronization system may affect the overall performance and stability of the system. Furthermore, the synchronization system should have a proper dynamic response in the case of grid faults in order to have a desired support from the DG in faulty conditions as well as to protect the DG. Therefore, the synchronizing signals are always affecting the control system, and by increasing the penetration of the converter-based DGs in the future power systems, it may threaten the overall system stability and reliability if not properly handled.

In addition to the synchronization at the start-up point and forming the reference sinusoidal waveforms for the control system, the grid voltage information is required for protection system such as over/under frequency, over/under voltage, and islanding detection. Moreover, the frequency of the grid is required for resonant controllers or filters as well as for reverse droop controller, the magnitude of the voltage is utilized by the control system to control the active and reactive power, and the harmonic contents can be used for passive anti-islanding algorithms, and active power filtering by power filters or multi-functional DG inverters.

Furthermore, the grid voltage at the coupling point is not a balanced pure sinusoidal signal with a fixed frequency, and it may be distorted by the non-linear loads as well as it is always unbalanced due to the single phase domestic, subway train, and industrial loads. Therefore, a precise synchronization algorithm is required for control and synchronization of the DGs and DSs.

### 1.1.2 Grid Synchronization Methods

Over the years, researchers have developed various methods to synchronize converter-based DGs with the grid. In the past, the focus of the research was on rejecting disturbances such as voltage harmonics, imbalances, phase jumps, and frequency deviations. However, there has been a shift in focus to enhancing synchronization stability in weak and faulty grids. This shift has been driven by the increasing reliance on converter-based resources in power systems, which can cause decreased stability due to reduced inertia and lower short circuit ratios (SCRs). As a result, the stability of converter-based DGs has become a major concern in modern power systems (Taul et al. 2019). In broad terms, the methods utilized for achieving grid synchronization can be bifurcated into two distinctive categories, based on the operational modes of converter-based DGs.

*The voltage-based grid synchronization:* The process of voltage-based grid synchronization involves measuring or estimating the frequency and phase of the voltage at the point where grid-connected converters are connected, also known as the point of common coupling (PCC). In some cases, voltage may be detected without the use of a voltage sensor. Once the phase is determined, it is used in conjunction with either vector current control or direct power control to regulate the exchange of active and reactive power between the converters and the grid. This method of grid synchronization is known as grid-following control, so named because it follows the phase of the grid voltage (Lasseter et al. 2019).

*The power-based synchronization:* By regulating the active power of converters, power-based synchronization controls the phase of the PCC voltage directly. The general approach is to use the active power-frequency ( $P-\omega$ ) droop control, which is commonly applied to synchronous generators, for converter synchronization with the grid. To monitor the generated phase of the PCC voltage, voltage control is necessary, which distinguishes this method from grid-following converters. Voltage-controlled converters are now referred to as grid-forming converters (Lasseter et al. 2019)

Due to the importance of the synchronization of the DGs/DSs in future power systems and its inherent effect on the overall stability, this chapter discusses the synchronization systems.

The paper is organized as follows. The GFL and GFM modes for power electronic interfaced DGs are discussed in Section 1.2. The grid synchronization methods for GFL converters including the basic PLL structure, different single-phase PLLs, improved PLLs for dc component rejection, and three-phase PLL techniques for unbalanced distorted grid voltages and harmonic compensation are explained in Section 1.3. Furthermore, some control algorithms for GFM inverters including droop control, droop control with low pass filters, and synchronous generators-based control are presented in Section 1.4.

## 1.2 Classification of Distributed Generations

DGs and DS systems can be categorized as dispatchable and non-dispatchable units as given Table I, where the output power of the dispatchable units can be controlled in the range of no load to full load. However, the non-dispatchable units can only be controlled from no load to the maximum power, which is determined by the prime resource like photovoltaic and wind energies. These units can only supply the maximum power into grid like a current source, and they are called GFL converters. The majority of the presently installed inverter-based DGs fit into this group, and, as such, voltage source behavior is not a fundamental feature of inverter-based DGs. In comparison to synchronous generators, the power electronic switching devices utilized in inverters have significantly lower over-current ratings. Consequently, inverter-based DGs are regarded as sources of non-synchronous generation. One of the primary difficulties associated with the growing integration of non-synchronous generation sources into power systems is the management of voltage and frequency regulation (Lin et al. 2020). The widely adopted method to achieve synchronization of GFL converters with the grid voltage is through the utilization of a phase-locked loop (PLL).

Microgrids have emerged as a platform for integrating inverter-based DGs, as they can operate in both grid-connected and islanded modes. In the grid-connected mode, the grid maintains frequency and voltage regulation; hence, inverter-based DGs function as grid-following inverters. In contrast, in the islanded mode, one or more inverters must operate as frequency and voltage regulators to establish a power grid. The development of GFM converters (dispatchable units) was initiated to meet this requirement. As the technology of microgrids progressed, it became apparent that it was necessary to simulate the functions of synchronous generators. Consequently, various enhancements, such as energy storage elements and control solutions (including virtual synchronous generator operation), were developed for GFM converters (Rathnayake et al. 2021). While the initial development of GFM converters was intended for their implementation in islanded microgrids, the applicability of this concept can extend to large-scale power systems, particularly in the integration of photovoltaic and wind units. As these renewable energy sources are usually situated in remote areas, the line impedance in these regions tends to be high, rendering them as weak sections of the grid. The traditional approaches to voltage control at the PCC become challenging in these weak grids. However, utilizing GFM converters offers a promising solution to this problem by strengthening the grid. The technology of GFM converters is still in its early stages of development. As a result, there is limited knowledge regarding the modeling methods, control approaches, challenges, and diverse applications of GFM converters.

A classification of GFL and GFM converters is shown in Fig. 1, and they are explained in the following subsections.

Table I: Classification of Different Distributed Sources and Storages

| <b>Source Type</b>            | <b>Specification</b> | <b>Example</b>                   |
|-------------------------------|----------------------|----------------------------------|
| <b>Distributed Generators</b> | Dispatchable         | Fuel Cell, Micro-Turbine         |
|                               | Non-dispatchable     | Photovoltaic, Wind Turbine       |
| <b>Distributed Storages</b>   | Dispatchable/Fast    | Battery                          |
|                               | Dispatchable/Slow    | Flywheel, Regenerative Fuel Cell |

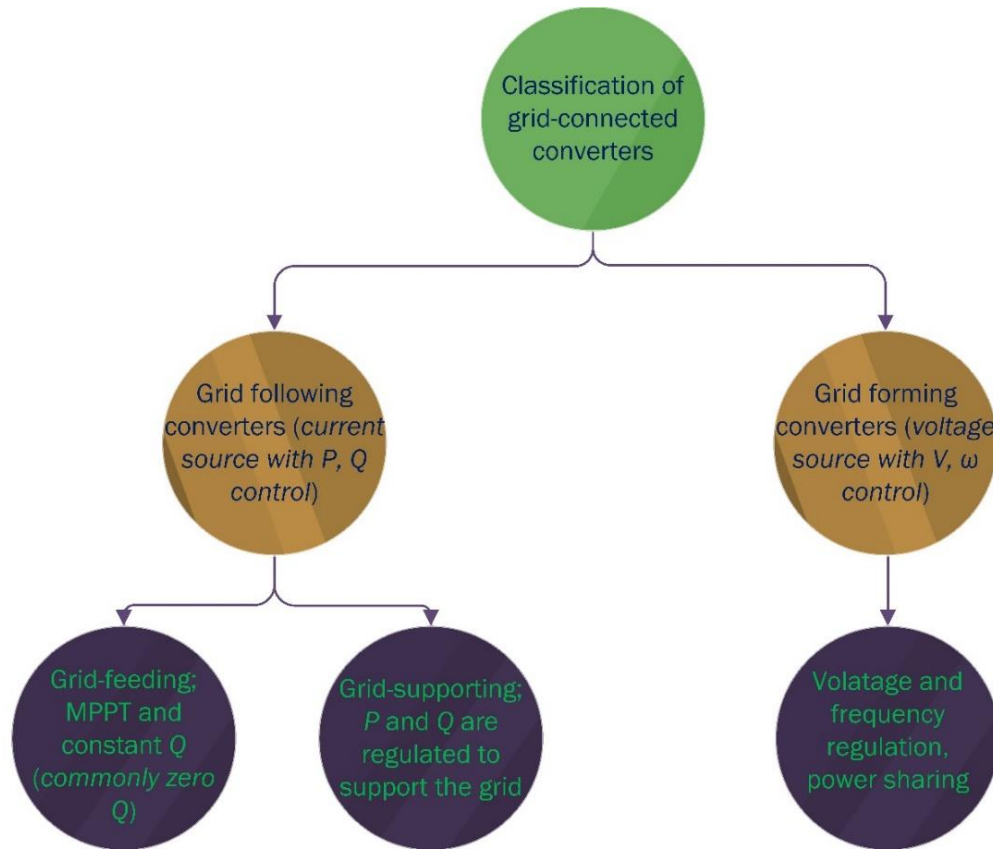


Fig. 1 Classification of grid-connected converters.

### 1.2.1 Grid Following DGs

The primary focus of GFL inverters applications is active power injection into the grid with maximum power point tracking (MPPT), resulting in a minimal reactive power supply often close to zero. These types of inverters are known as grid-feeding inverters. Although it is more attractive from a revenue perspective to operate inverter-based DGs as GFL inverters, the increased number of GFL inverters presents challenges for voltage and frequency regulation. As a result, the grid operators have mandated stringent regulations on inverter-based DGs that are large in scale, usually exceeding 5 MW, to provide reactive power support and adjust active power output in response to grid fluctuations. Inverter-based DGs that operate in the grid supporting mode are known as grid-supporting inverters (Rathnayake et al. 2021).

The GFL inverters can be modeled as an ideal current source as shown in Fig. 2 (a), which injects the reference power into the grid. In the case of grid feeding DGs, the voltage reference is dictated by the grid at the coupling point. These DGs only follow up the grid frequency and phase angle to appropriately supply the desired power into the grid. Photovoltaic arrays and wind turbines are controlled in the grid feeding mode to feed the maximum power into the grid. In these kind of sources, the reference of the active power ( $P^*$ ) is determined by the MPPT, and the set point of reactive power ( $Q^*$ ) can be chosen to achieve a desired power factor, or it can be determined by the Transmission System Operator (TSO) or the Distribution System Operator (DSO). A general approach of a control system of a three phase grid feeding inverter implemented in the  $dq$  reference frame is shown in Fig. 3 (Rocabert et al. 2012). In order properly to supply the reference active and reactive power into the grid, a synchronization system needs to follow up the grid phase angle. For example, in Fig. 3, the phase angle of the PCC's voltage is estimated by employing a PLL. In this type of DGs,

the synchronization system always interacts with the control system. Hence, the accurate and dynamically fast synchronization algorithms have to be employed to guarantee the system stability.

The general three phase approach in the stationary reference frame is also shown in Fig. 4. In this approach the  $abc$  to  $\alpha\beta$  transform is used to convert the three phase voltage  $v_{abc}$  and current  $i_{abc}$  into the stationary frame. The instantaneous power theory (Akagi et al. 2007) may then be employed to define the reference currents for the control loop to track the input active and reactive power. In this frame, the synchronization system can be removed. However, in the case of distorted grid voltage, the performance of the converter may be deteriorated. The basic single phase control for photovoltaic applications is also shown in Fig. 5, where a PLL is utilized to synchronize the output current to the grid voltage. The active power (current) reference is determined by the MPPT system.

The GFL inverters that operate in the grid supporting can be controlled in reverse droop mode, like the one shown in Fig. 6. Reverse droop controlled DGs, also called current source DGs, cannot form the voltage and frequency of the grid and they should be connected to a grid with at least one grid forming or grid supporting voltage source converters. As it can be seen from Fig. 6, the frequency and the phase angle employed by the control system of the current source converters are dictated by the grid, and hence, a synchronization system is necessary to estimate the grid phase angle for the current controllers as well as grid frequency and voltage amplitude for the droop controller. Therefore, a precise synchronization algorithm is required not only to estimate the grid phase angle but also to accurately extract the grid frequency. Since the voltage and frequency are imposed by the grid, these DGs are called current source converters and can be modeled like a current source, and the droop approach is nominated as reverse mode droop. In the future, by increasing the penetration of the wind turbines and photovoltaic arrays, they should participate in frequency supporting of the grid. Therefore, they need to operate at a power lower than the MPPT power (e.g., 90% of the MPPT power). The remaining power is considered as a reserve for frequency support. The supported power by the parallel current source converters is shared according to the corresponding droop gains ( $k_p, k_q$ ).

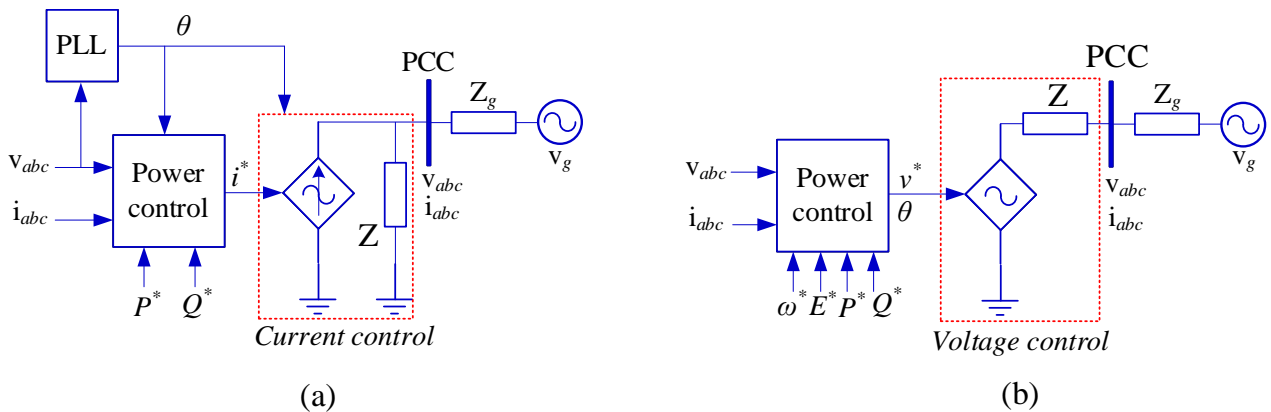


Fig. 2 Comparison of control and approximation of (a) GFL inverter and (b) GFM inverter



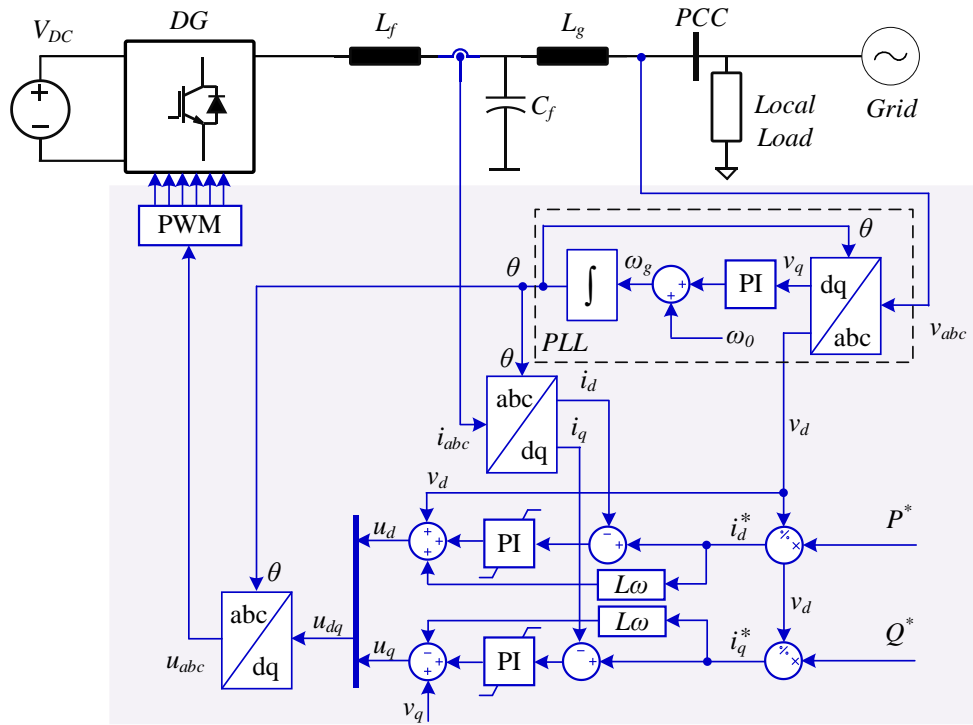


Fig. 3. Basic control structure of a three phase grid feeding converter in synchronous reference frame, generating the reference active  $P^*$  and reactive  $Q^*$  powers. The PLL is the grid synchronization unit –  $L = L_g + L_f$ .

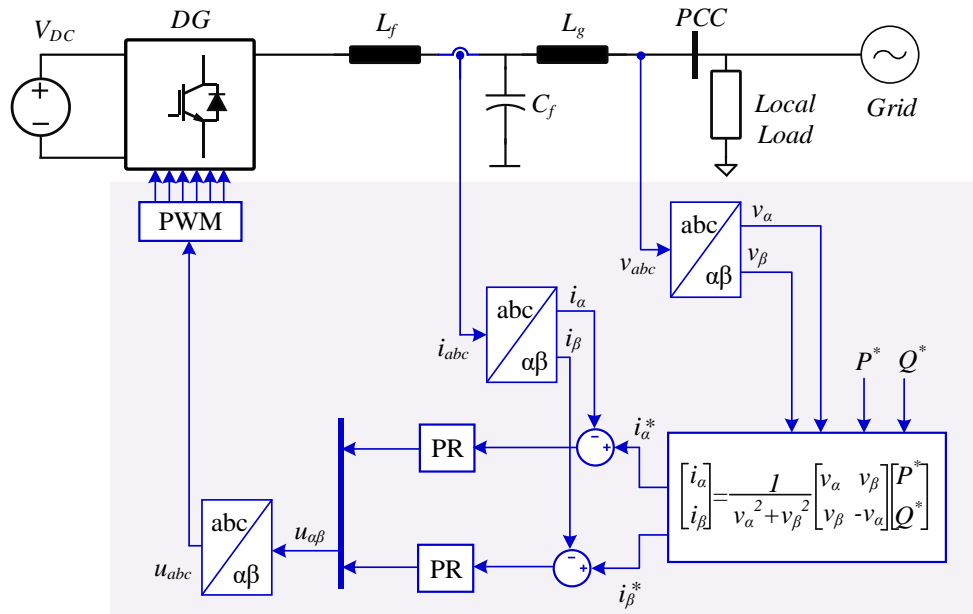


Fig. 4. Basic control structure of a three phase grid feeding converter in stationary reference frame, generating the reference active  $P^*$  and reactive  $Q^*$  powers.

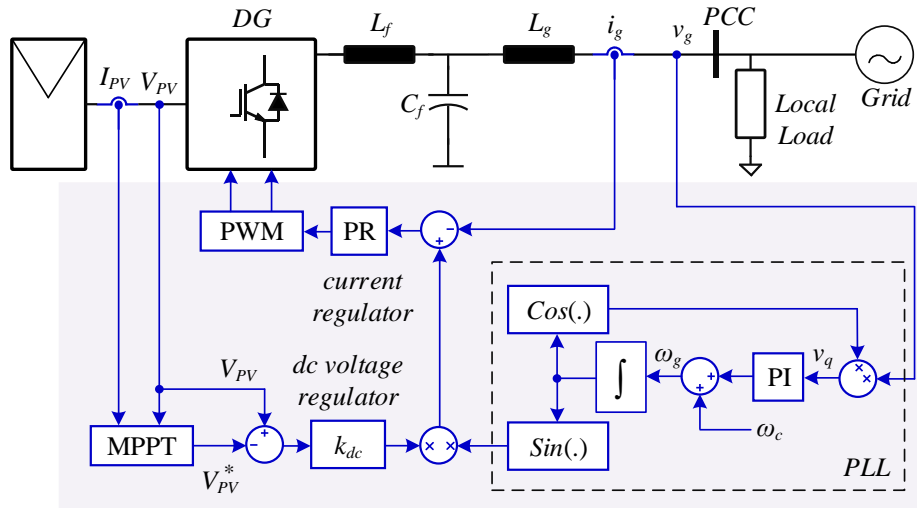


Fig. 5. Basic control structure of a single-phase grid feeding converter for grid connected photovoltaic array.

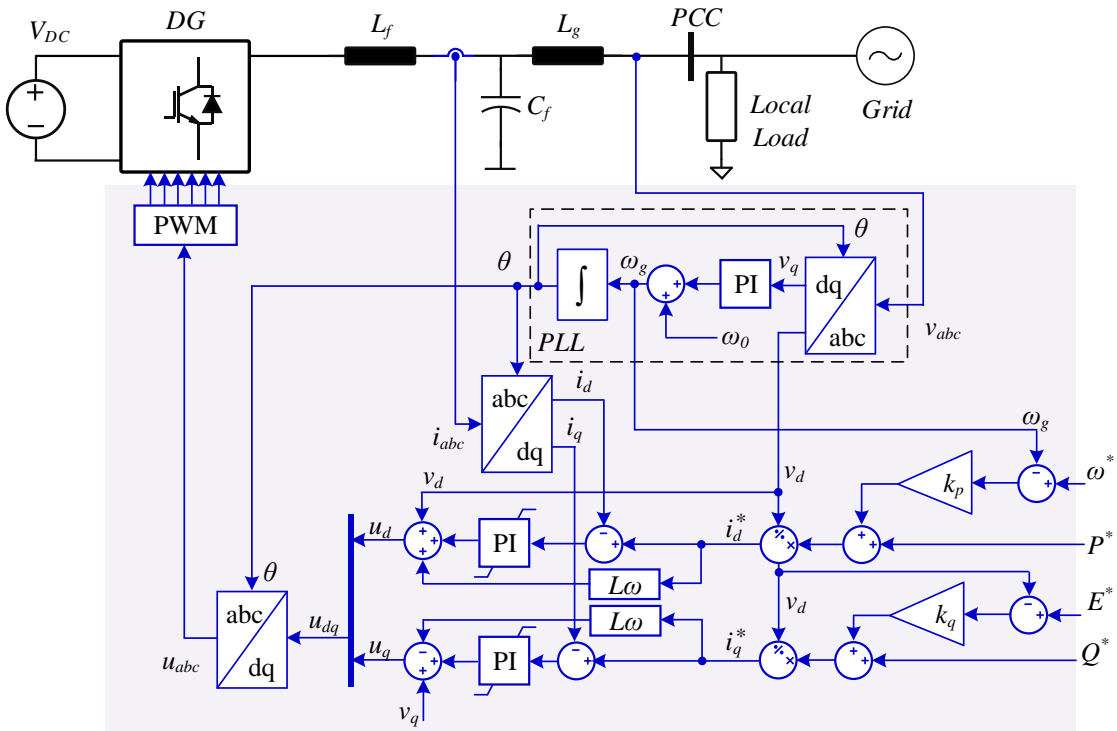


Fig. 6. Basic control structure of a three phase grid supporting current source converter with reverse droop control –  $L = L_g + L_f$ .

### 1.2.2 Grid Forming DGs

GFM DGs are anticipated to function similarly to synchronous generators. Therefore, it is crucial to replicate the significant attributes of synchronous generators, including the capacity to provide constant or committed power to the grid, exhibit inertial response, and maintain fault current behavior to the greatest extent feasible. To ensure a steady delivery of committed power, some form of energy storage is essential, regardless of any variations in the input of wind or solar power. Likewise, to achieve the required response duration for inertial response, energy storage is also necessary. GFM DGs are responsible for generating the voltage of the

grid. They are, in practice, supplied by a stable source such as batteries, fuel cell modules, and micro-turbines. The amplitude and frequency of the grid are determined and controlled by the grid forming DGs, and hence, they form the reference for the other DGs. A general control block diagram of a GFM converter is shown in Fig. 7 (Rocabert et al. 2012). The amplitude and frequency of the output voltage ( $v_{abc}$ ) are determined by a nominal amplitude  $E^*$  and nominal frequency  $\omega^*$ . The three-phase balanced sinusoidal ac voltage  $u_{abc}$  is generated by two cascaded synchronous controllers in the  $dq$  reference frame. The phase angle of the ac voltage is formed by integrating the nominal frequency. These type of DGs are operated as an ideal voltage source, and hence, the power sharing among different GFM DGs is a function of their output impedances as well as inertied line impedances. Parallel operation of the GFM DGs requires a precise synchronization system at the start-up point. In the islanded mode of operation, the synchronization system should oscillate at the nominal frequency  $\omega^*$  to form the output voltage. During the connection to the grid, grid forming converters need to be synchronized with the grid. Therefore, the synchronization system should slowly change the frequency ( $\omega^*$ ) and the phase angle ( $\theta$ ) to synchronize with the grid. During the islanding, the synchronization system needs to detect the islanding condition, and accurately provide the synchronization signals to the DG in order to form the voltage of the local grid (Rocabert et al. 2012). Unlike GFL converters, a GFM converter operates as a voltage source, which aligns with the power grid through the active and reactive power controls, as depicted in Fig. 2(b). As a result, the PLL is unnecessary for grid synchronization of grid-forming converters during regular operations.

The GFM inverters that operate in the grid supporting can be controlled based on the droop approach of the conventional synchronous generators, as shown in Fig. 8. They form their output voltage without employing the grid voltage information, and hence, they can operate in both grid connected and islanded mode of operation. Based on the droop mechanism, these converters can find the frequency and phase angle by regulating their output power. They should only be synchronized with the grid at the start-up point. During the operation, any load and frequency variation can be supported by the droop controller. Moreover, the power sharing among the voltage source converters is performed according to the corresponding droop gains ( $k_p, k_q$ ). The GFM inverter control methods are discussed in Section 1.4.

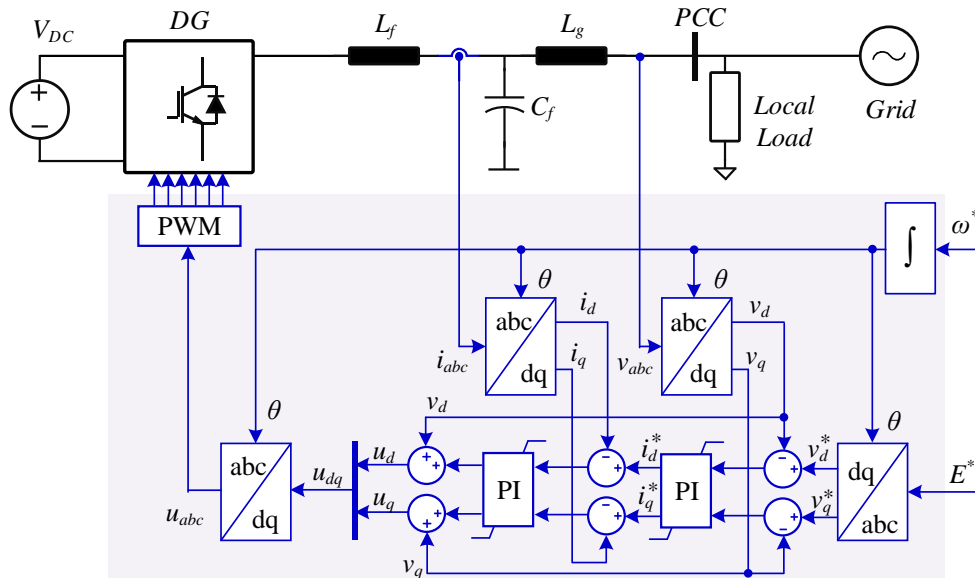


Fig. 7. Basic control structure of a three phase grid forming converter generating an ac voltage with nominal amplitude  $E^*$  and nominal frequency  $\omega^*$ .

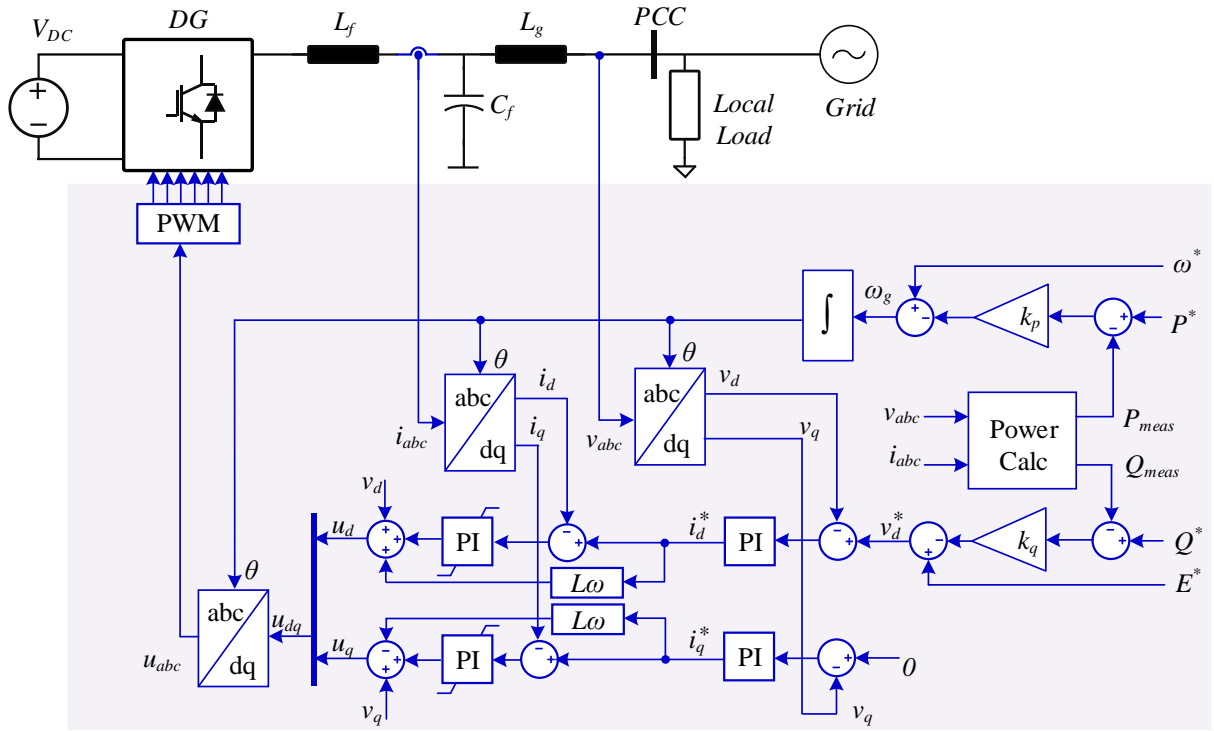


Fig. 8. Basic control structure of a three phase grid supporting voltage source converter with forward droop control –  $L = L_g + L_f$ .

### 1.2.3 Performance comparison between GFL and GFM inverters

Unlike GFL inverters, which measure  $v_{abc}$  for synchronization purposes, GFM inverters form a  $v_{abc}$  to regulate their power output. Additionally, a significant difference between GFL inverter and GFM inverter control is that GFM inverter can operate and supply power to local loads even without a grid connection by establishing its own reference voltage and frequency (Unruh et al. 2020). During steady-state operation, GFL and GFM inverters can both inject active and reactive power into the grid based on control topology, power set-points, and grid conditions. However, when dealing with weak grids, the most notable difference in performance between these inverters is their response to a grid disturbance. Both GFL and GFM inverters can provide active and reactive power support during a disturbance, which is also known as virtual or emulated inertia support, depending on the source type. While a GFL inverter measures the disturbance through voltage and current measurements and takes appropriate control actions for grid support functionality, its active or reactive power response is associated with a certain degree of control delay and measurement. Nevertheless, since the internal voltage phasor of the GFM inverter remains unaffected at the start of a disturbance, the power output can respond instantly, provided that the grid angle changes quickly. However, while the GFM inverter response time is significantly faster than that of the GFL inverter, it is necessary to address concerns regarding stability and current limitations when responding rapidly. The control of the GFM inverter and GFL inverter differ in terms of their performance regarding small-signal stability under weak grid conditions. GFLs rely on grid angle measurements and voltage to stay synchronized with the grid, which can significantly reduce the stability margin when there are sudden changes in the measured grid signals. On the other hand, GFMs address this issue by offering self-synchronization and operating synchronously without depending on grid signals (Unruh et al. 2020).

### 1.3 Grid-synchronization methods– GFL inverters

In this section, single phase and three phase grid synchronization algorithms are presented. Moreover, improved synchronization algorithms for dc rejection, harmonic compensation, and positive/negative sequence decomposition are discussed.

#### 1.3.1 Single Phase – PLL

The main objectives of grid monitoring techniques including Zero Crossing Detection (ZCD) methods and PLL algorithms are to extract the phase angle and amplitude of the input voltage. ZCD methods are implemented without phase controller, and they estimate the grid frequency every zero crossing points i.e., every half cycle of the line frequency. The major drawbacks of the ZCD methods include slow dynamic response and poor performance in the case of harmonic polluted signals. To overcome the mentioned issues, some improved ZCD algorithms have been presented (Valiviita 1999). However, these algorithms introduce more complexity, and they may not be suitable for applications which require high accuracy and fast dynamic response. Therefore, Phase Locked Loop (PLL) algorithms are introduced in order to precisely track the fundamental frequency, detect the frequency variation, and filter the harmonics with fast response. The PLL algorithms are more robust and resilient in respect to the grid voltage fluctuations and distortions. In the following, the basic structure of PLL and different single phase PLL algorithms are explained.

#### 1.3.2 Basic Structure of a PLL

PLL based algorithms, employs a Proportional-Integrator (PI) phase controller, which introduce high accuracy and fast dynamic response. The basic structure of a PLL as shown in Fig. 9, which consist of two main blocks including Low-Pass Filter (LPF) as a PI controller in order to attenuate the high frequency ac component of the input signal, and Voltage-Controlled Oscillator (VCO) for generating a sinusoidal signal ( $v$ ), whose frequency is close to the center frequency ( $\omega_c$ ) provided by the LPF. A block diagram of an elementary PLL structure is shown in Fig. 10, where the LPF is a PI controller and a VCO generates a sinusoidal voltage ( $v$ ) with the shifted frequency of ( $\omega_g$ ). The estimated signal ( $v$ ) is the shifted form of the input signal ( $v_g$ ) by  $\pi/2$  rad. Generating the orthogonal signal by a cosine function makes a high frequency component twice the grid frequency (Teodorescu et al. 2011; Karimi-Ghartemani 2014), which affects and limits the bandwidth of the PLL, and hence, its dynamic performance is slow for grid connected applications. In order to solve this problem, some Orthogonal Signal Generators (OSGs) have been presented. The orthogonal component of the input signal does not have a frequency component at twice the line frequency, which implies a higher performance of the PLLs employing the OSG methods rather than the previous one.

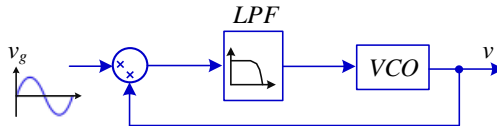


Fig. 9. Basic structure of a PLL.

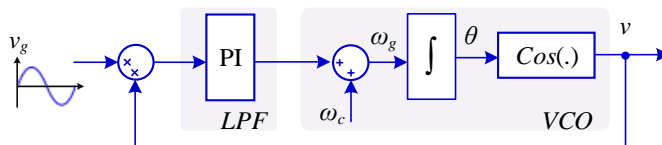


Fig. 10. An elementary structure of a PLL.

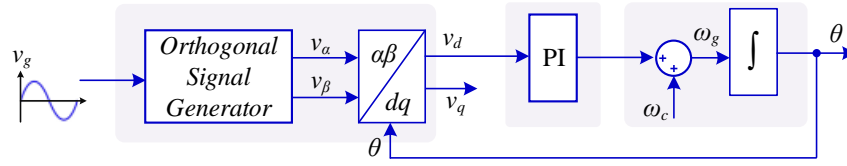


Fig. 11. QSG based PLL employing Park transformation – VSO uses the d axis component.

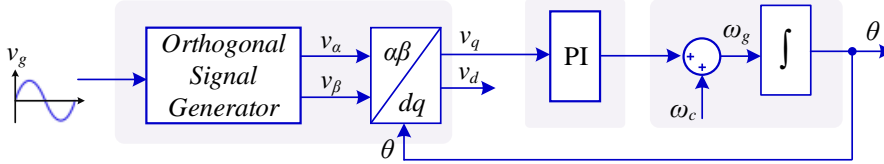


Fig. 12. QSG based PLL employing Park transformation – VSO uses the q axis component.

### 1.3.3 OSG Based PLL

The basic structure of orthogonal Signal Generator (OSG) based PLLs are shown in Fig. and Fig. . An OSG block generates two quadrant  $\alpha\beta$  components, where  $\alpha$  component ( $v_\alpha$ ) is in phase with the input signal, and the  $\beta$  component ( $v_\beta$ ) is the shifted form of the input signal by  $\pi/2$  rad. The Park transformation is employed to convert the ac signals into the dc signals in the  $dq$  reference frame. Either the  $d$ -axis or  $q$ -axis component can be used by the PLL to estimate the phase angle of the input signal. Some OSG algorithms are presented in the following.

#### 1.3.3.1 Transport Delay Based OSG PLL

A simple way to generate the orthogonal signals is to shift the input signal by  $T/4$  as shown in Fig. , where  $T$  is the period of the fundamental frequency ( $\omega_c$ ). This method is only suitable for pure sinusoidal signals with a nominal frequency. However, this method is not applicable for the droop controlled systems with a variable frequency.

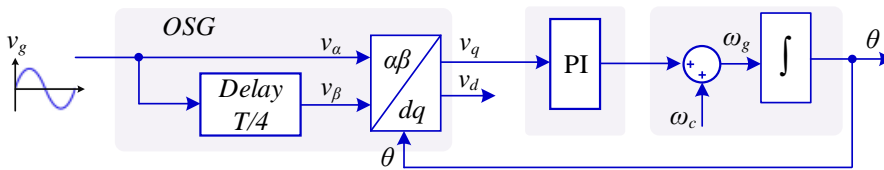


Fig. 13. PLL based on a T/4 transport delay.

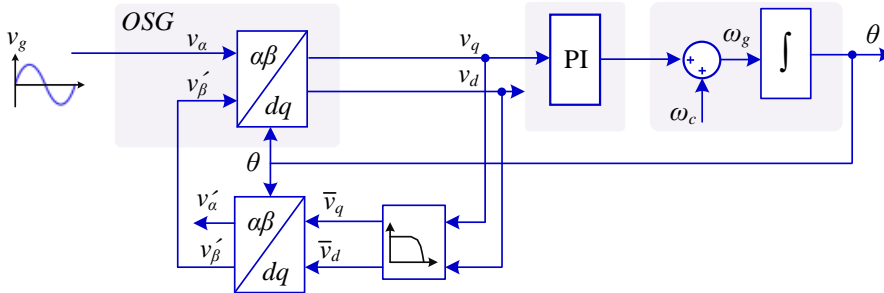


Fig. 14. PLL based on the inverse Park transform.

### 1.3.3.2 Inverse Park Transform Based PLL

Another approach to generate the orthogonal signals is using the inverse Park transform as shown in Fig. . If the PLL is not synchronized with the input signal, the output signals of the forward Park transform will have oscillations, which will be attenuated by utilizing the LPFs. Therefore, the output signals of the inverse Park transform will be orthogonal. Once the PLL finds the phase angle, the input signals of the forward Park transform will be orthogonal. Although the PLL based on the inverse Park transform is easy to implement in practice, tuning the PI controller and selecting the time constant of the LPFs are difficult due to the interdependent non-linear double loop systems (Teodorescu et al. 2011).

### 1.3.3.3 Filter Based PLL

In order to produce the orthogonal component of the input signal, three approaches based on filtering the input voltage are given in Fig. , and Fig. . A second order filter based PLL is shown in Fig. , making  $\pi/2$  rad phase shift in the input voltage. The natural un-damped frequency ( $\omega$ ) of the filter can be tuned by the estimated frequency ( $\omega_g$ ), and hence, the performance of the system is not affected by the grid voltage variation (Choi et al. 2006). The all-pass filter shown in Fig. , can also be used to generate the orthogonal component of the input voltage. The natural un-damped frequency ( $\omega$ ) of the filter can be tuned by the estimated frequency ( $(\sqrt{2} - 1)\omega_g$ ). However, as mentioned in (Choi et al. 2006), the performance of the second order filter based PLL is better than the first order filter and the all-pass filter.

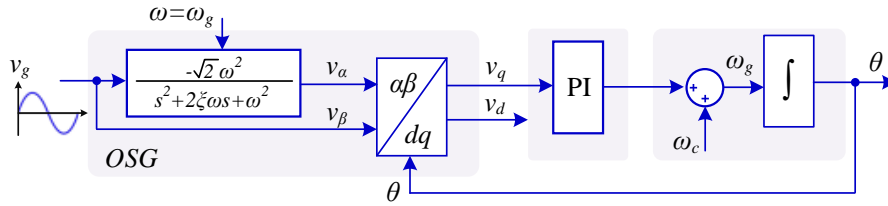


Fig. 15. PLL based on second order filter OSG.

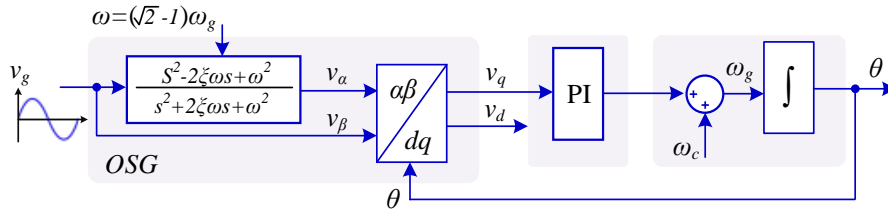


Fig. 16. PLL based on all-pass filter OSG.

### 1.3.3.4 SOGI PLL and Frequency Locked Loop (FLL)

A Second Order Generalized Integrator (SOGI) based PLL is shown in Fig. . The SOGI PLL is a second order filter based system, and the transfer functions from input to the orthogonal components (i.e.,  $v_\alpha, v_\beta$ ) can be obtained as:

$$\frac{v_\alpha}{v_g} = \frac{k\omega s}{s^2 + k\omega s + \omega^2}, \quad (1)$$

$$\frac{v_\beta}{v_g} = \frac{k\omega s}{s^2 + k\omega s + \omega^2}, \quad (2)$$

where  $v_g$  is the input voltage,  $k$  is the half of the damping ratio, and  $\omega$  is the un-damped natural frequency. As it can be seen in Fig. , the tuning frequency of the second order filter is updated to the estimated frequency  $\omega_g$  provided by the PLL, and hence, the performance of the PLL cannot be affected by the grid voltage fluctuations. Therefore, the SOGI-OSG provides the filtered orthogonal components for the PLL, without filtering delay, and high performance due to the online frequency adaption (Teodorescu et al. 2011).

Another approach based on SOGI-OSG, which can estimate the frequency of the input voltage, is the SOGI Frequency Locked Loop (SOGI-FLL) as shown in Fig. (Teodorescu et al. 2011). The inherent resonant capability of the SOGI-OSGI makes it to work as a VCO and provides an opportunity to estimate the grid frequency and phase angle with improved performance.

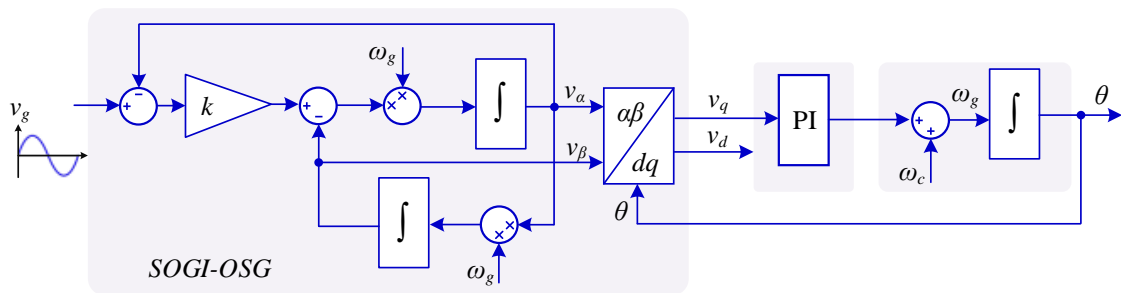


Fig. 17. Block diagram of the SOGI based PLL (SOGI-PLL).

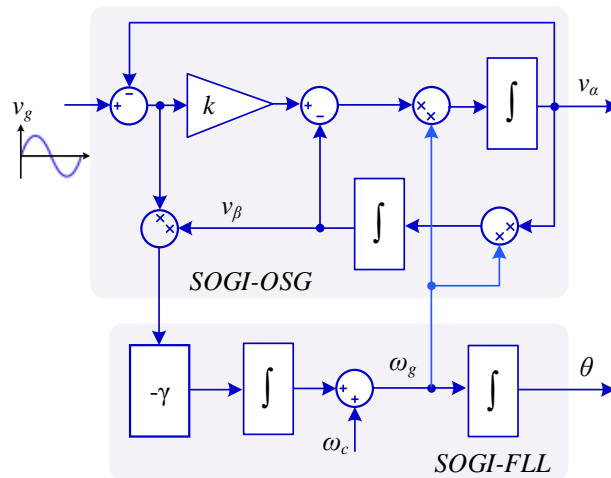


Fig. 18. Block diagram of the SOGI based FLL (SOGI-FLL).



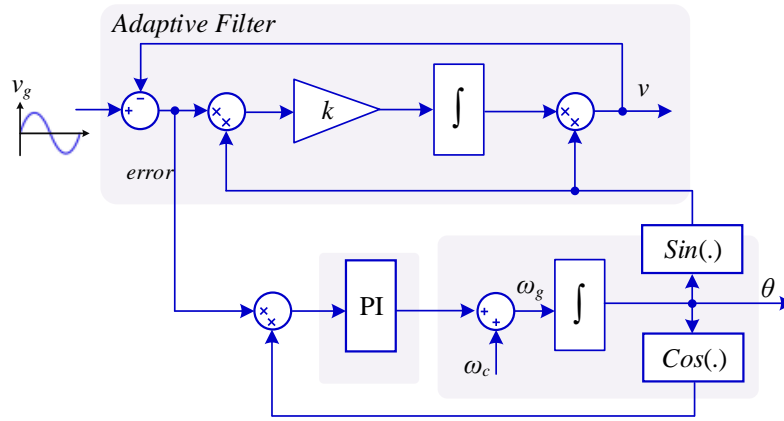


Fig. 2. Block diagram of Enhanced PLL (EPLL)

### 1.3.3.5 Enhanced PLL

Enhanced PLL (EPLL) proposed by (Karimi-Ghartemani & Iravani 2001; Karimi-Ghartemani 2014), improves the performance of the conventional PLL by an adaptive filter shown in Fig. 2. In fact, the adaptive filter estimates the fundamental component of the input voltage ( $v$ ), and improves the conventional PLL drawback by removing the double frequency ripple from the input error. The positive constant  $k$  is a control parameter, and the control design is discussed in (Karimi-Ghartemani & Iravani 2001; Karimi-Ghartemani 2014).

### 1.3.4 DC Component Rejection

In practice, dc component may be appealing in the input signal ( $v_g$ ) which can be introduced by measurement units, the analog to digital conversion process and etc. The dc component may affect the PLL performance. Some improved PLLs are presented for dc rejection in the following.

The improved structure of the SOGI-FLL is shown in Fig. 20 (Karimi-Ghartemani et al. 2012). The dc rejection path is highlighted in red and can estimate the dc term, and then, subtracted from the input voltage. Therefore, the input signal of the FLL is dc-free signal, and it can estimate the frequency without any error.

Another dc rejection technique is presented by (Ciobotaru et al. 2008), based on the SOGI-PLL. In the SOGI-OSG, the dc is only appealing in the orthogonal component of the input signal. Hence, as it can be seen in Fig. 21, the dc term can be removed from the orthogonal component through an LPF.

Furthermore, the EPLL can also remove the dc offset by an additional path shown in Fig. 22 (Karimi-Ghartemani et al. 2012). The dc offset can be estimated by a weighted integrator and subtracted from the input signal. As mentioned, dc rejection algorithms are only viable for a small dc offset induced by the measurement units or the digital signal processors. However, large dc components cannot be removed by the proposed approaches. In the other words, if the frequency and phase angle of an ac ripple in the dc voltage is desired, most of the PLL structures are not able to estimate the frequency and phase angle with an acceptable dynamic response.

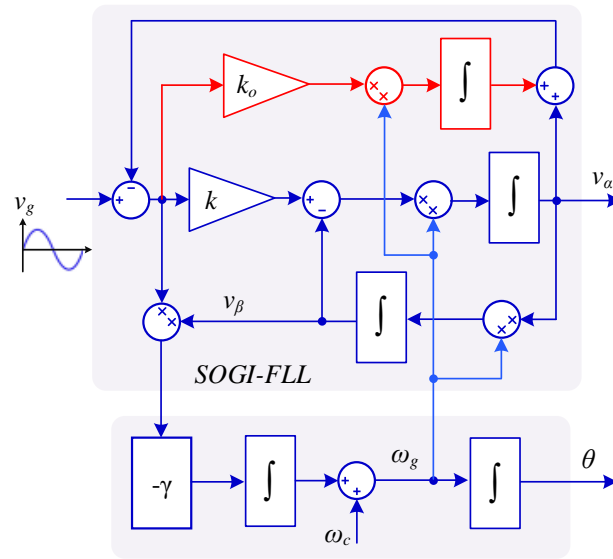


Fig. 20. Block diagram of the SOGI based FLL (SOGI-FLL) with dc rejection capability.

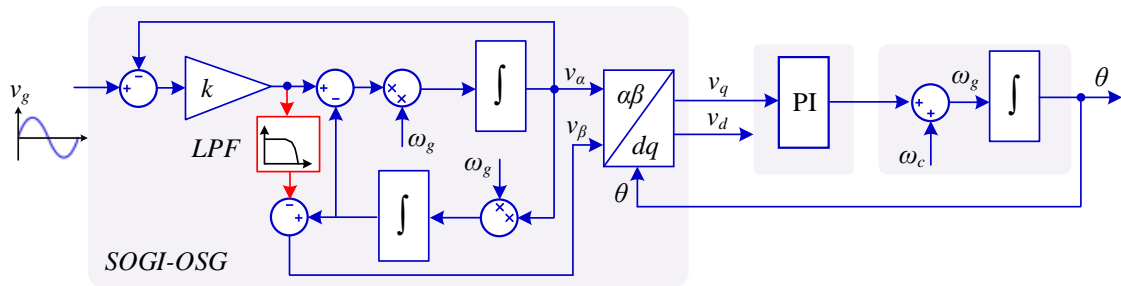


Fig. 21. Block diagram of the SOGI based FLL (SOGI-FLL) with dc rejection capability.

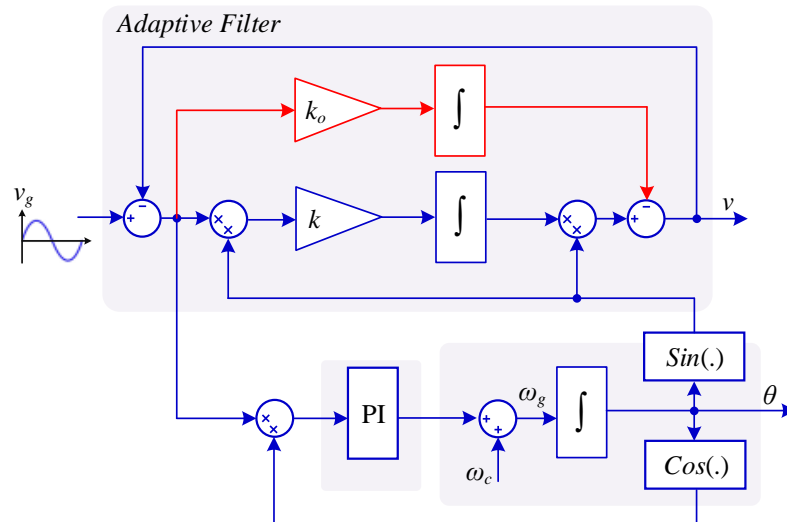


Fig. 22. Block diagram of the Enhanced PLL (EPLL) with dc rejection capability.

### 1.3.5 Three Phase – PLL

In order to synchronize a three-phase converter-based DG to the utility grid and properly control the converter at different loading conditions and distorted grid voltage, an appropriate three phase synchronization system is required. Three phase PLL structures are used to make a synchronization in three phase DGs which are explained in the following.

### 1.3.6 Basic Structure of PLL

The conventional PLL structure at Synchronous Reference Frame (SRF) is shown in Fig. 23, where the  $q$  axes component ( $v_q$ ) of the grid voltage ( $v_{abc}$ ) is used to estimate the grid phase angle ( $\theta$ ). The SRF-PLL can properly estimate the phase angle and frequency in the case of balanced and pure grid voltage. However, the performance of the SRF-PLL under unbalanced and distorted grid condition is not acceptable, and the system may lose the controllability and make an interaction with the grid (Karimi-Ghartemani 2014; Teodorescu et al. 2011).

### 1.3.7 Synchronous Reference Frame PLL for Unbalanced and Distorted Grid Voltage

In the case of unbalanced and distorted grid voltage condition, especially in grid faults, the conventional SRF-PLL has not enough performance to estimate the grid information. Therefore, some techniques are required to extract the positive component of the grid voltage. Some improved SRF based PLL algorithms are presented in (Timbus et al. 2006; Benhabib & Saadate 2005; Karimi-Ghartemani & Iravani 2004) in order to decompose the positive sequence of the unbalanced voltage. However, the performance of the presented techniques in the case of distorted grid voltages is not acceptable.

In order to estimate the frequency and phase angle of a distorted and unbalanced grid voltage, a high performance technique on the SRF is presented in (Rodriguez et al. 2007). As shown in Fig. 24, two decoupled SRFs are used to decouple the positive and negative sequences. This method, also called Decoupled Double Synchronous Reference Frame (DDSRF), can estimate the phase angle by utilizing a conventional PLL. As it can be seen from Fig. 24, and Fig. 25, this method extracts exactly the positive and negative sequences, and hence, the performance of the method is enhanced in the case of distorted and unbalanced grid conditions.

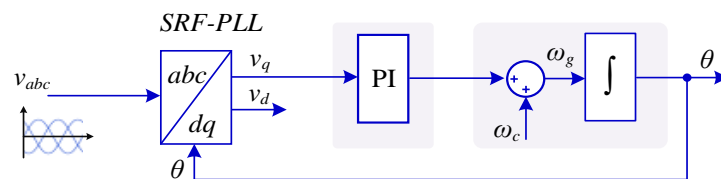


Fig. 23. Basic structure of a Synchronous Reference Frame (SRF) PLL.

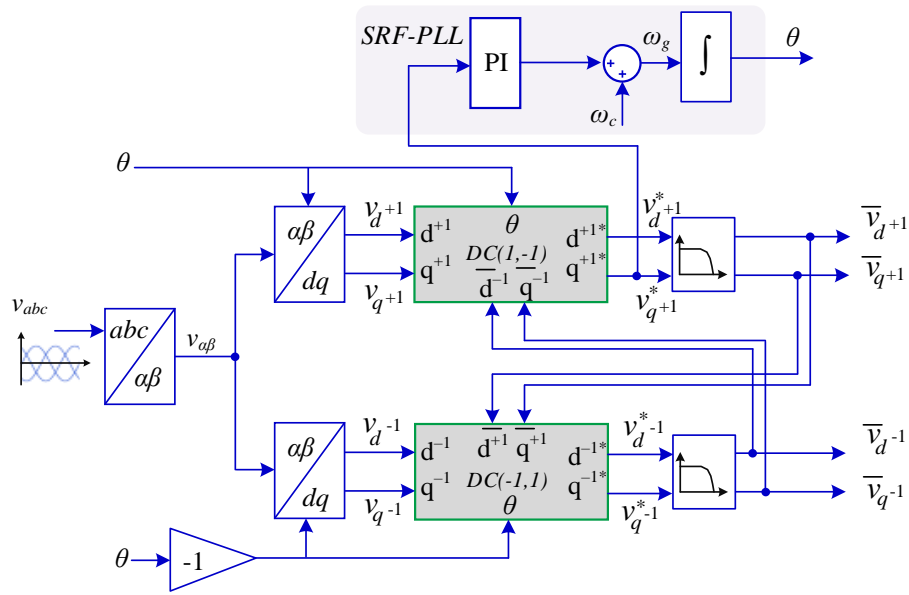


Fig. 24. Block diagram of Decoupled Double Synchronous Reference Frame (DDSRF) based PLL.

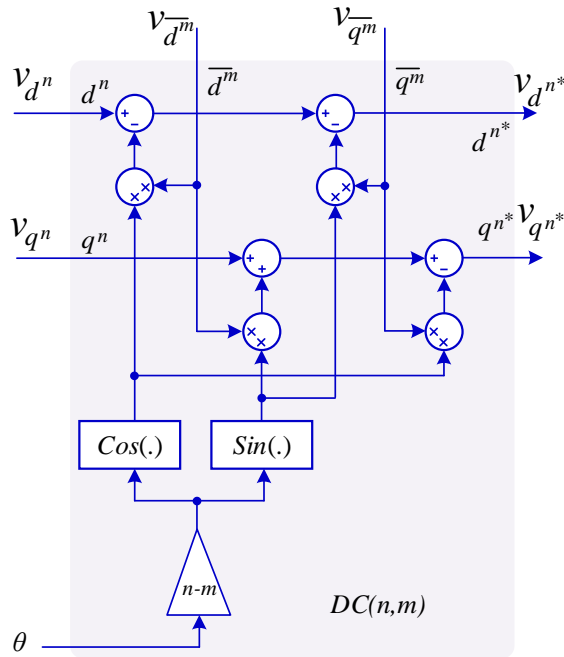


Fig. 25. Block diagram of the decoupling cell in DDSRF for blocking the effect of the  $n^{th}$  component on the  $m^{th}$  dq frame.

### 1.3.8 Stationary Reference Frame Double SOGI PLL for Unbalanced Grid Voltage

A three phase Double SOGI FLL (DSOGI-FLL) for unbalanced grid conditions is shown in Fig. 26 (Rodríguez et al. 2011), where the two SOGI-OSGs are employed for  $\alpha$  and  $\beta$  axes. The FLL is utilized to estimate the frequency and phase angle of the positive component of the input signal. The performance of the DSOGI-FLL is better than that of the DDSRF-PLL, since the FLL is less sensitive compared to the PLL in respect to the phase angle jumps in the grid voltage, which may introduce a fast dynamic response and smooth transition between islanding and grid connected modes. However, unlike the DDSRF-PLL, DSOGI-FLL is not

able to remove the effect of low order harmonics from the input voltage, and the performance of the DSOGI-FLL is not acceptable in the case of distorted grid voltages.

In order to overcome this problem, Multi-resonant SOGI FLL (MSOGI-FLL) is proposed by (Rodríguez et al. 2011). In this approach, the DSOGI-OSG blocks are used for every harmonic order to decompose from the input voltage with the estimated frequency of the FLL multiplied by the harmonic order. Hence, the performance of the DSOGI-FLL is improved and it can be used for unbalanced distorted voltages with better dynamic response compared to the DDSRF-PLL. Furthermore, three phase EPLL structures to decompose the harmonic and negative sequence of the distorted and unbalanced grid voltage are discussed in (Karimi-Ghartemani 2014).

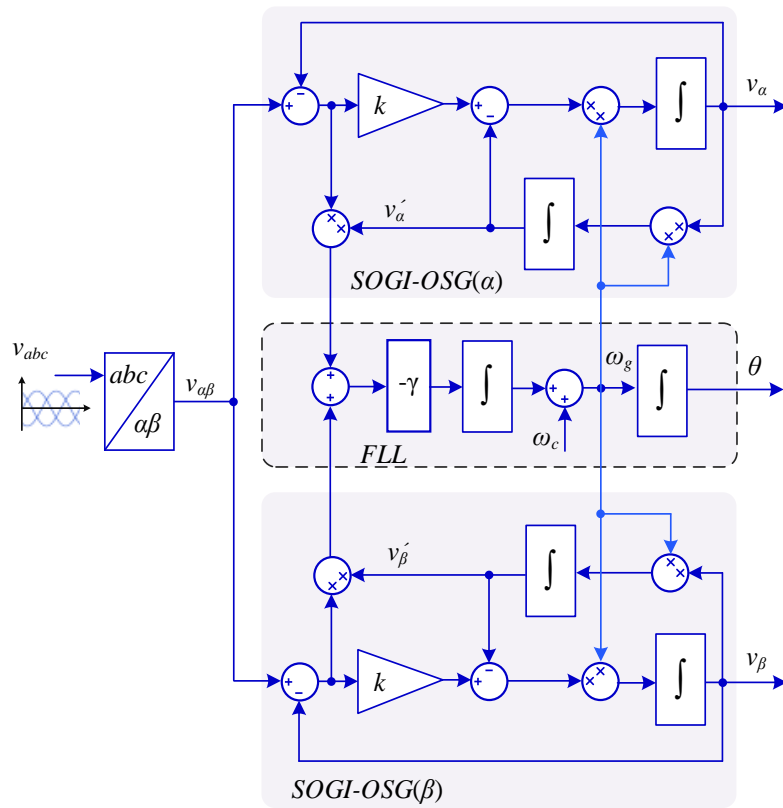


Fig. 26. Block diagram of DSOGI-FLL.

### 1.3.9 Synchronization for Power Quality Improvement

As DGs are operated near the load, they can compensate the load harmonics as an active power filter. Therefore, in addition to the active and reactive power, a multi-functional DG needs to be controlled to provide power quality services to the grid. In order to compensate the non-linear load harmonics, the synchronization system should extract the distorted components of the current. In this regard, two general control approaches are represented in Fig. and Fig. , respectively in the SRF and stationary reference frame. As it can be seen from Fig., for the 5<sup>th</sup> order harmonic compensation in the SRF, four transform functions and two PI controllers as well as two LPFs and two High Pass Filters (HPFs) are required. Moreover, in the case of unbalanced systems, two times more than the mentioned calculations are required. Considering the other harmonics in e.g., 7<sup>th</sup>, 11<sup>th</sup>, ..., a complicated control system should be implemented in practice (Blaabjerg et al. 2006).

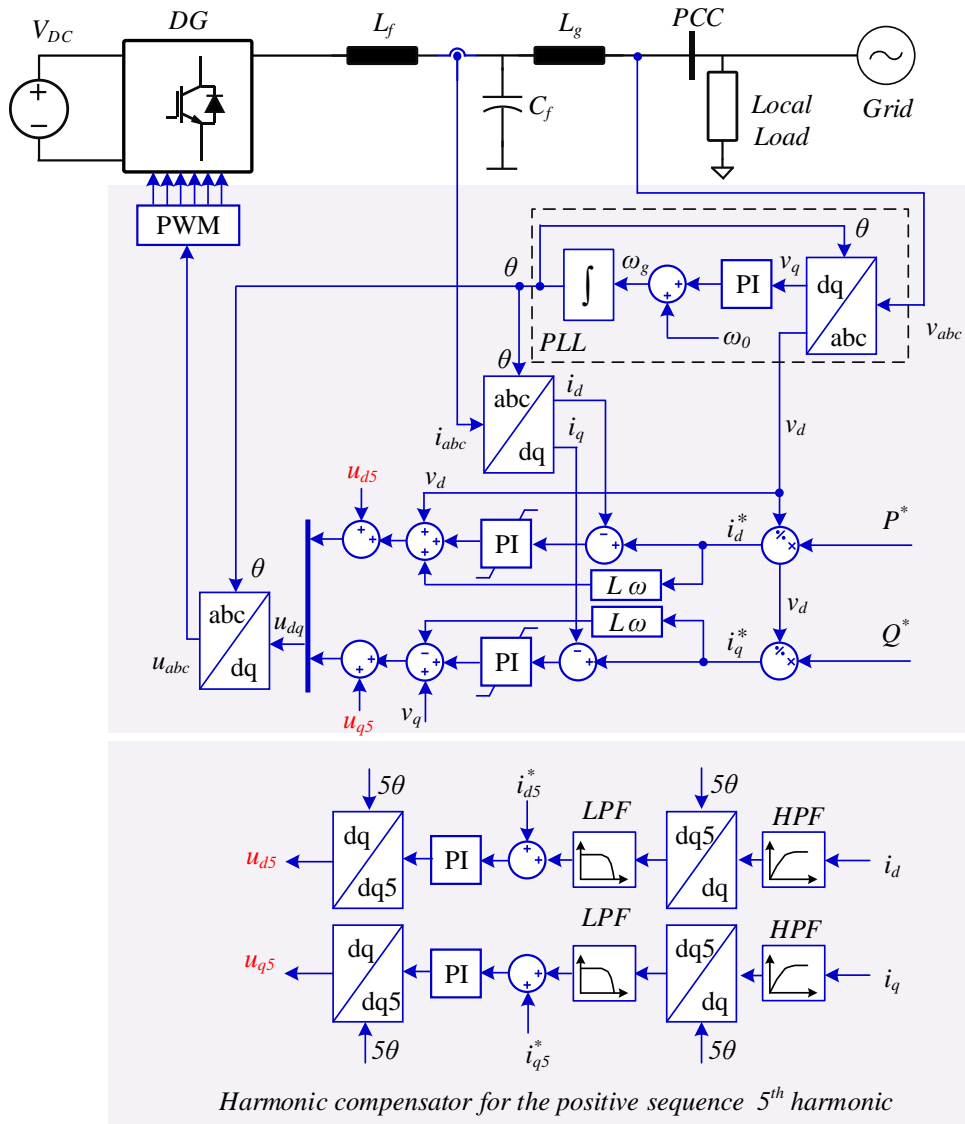


Fig. 27. Basic control structure of a three phase grid following converter generating the reference active  $P^*$  and reactive  $Q^*$  powers with harmonic compensation of the 5<sup>th</sup> order harmonic in the dq reference frame –  $L = L_g + L_f$ .

However, the control system in stationary reference frame shown in Fig. , are based on a generalized integrator for balanced and unbalanced systems, without using extra transformation and LPFs/HPFs, and

hence, it is easy to implement (Blaabjerg et al. 2006). In this approach, the resonance frequency of the generalized integrator can be tuned by the estimated frequency ( $\omega_g$ ) of the PLL.

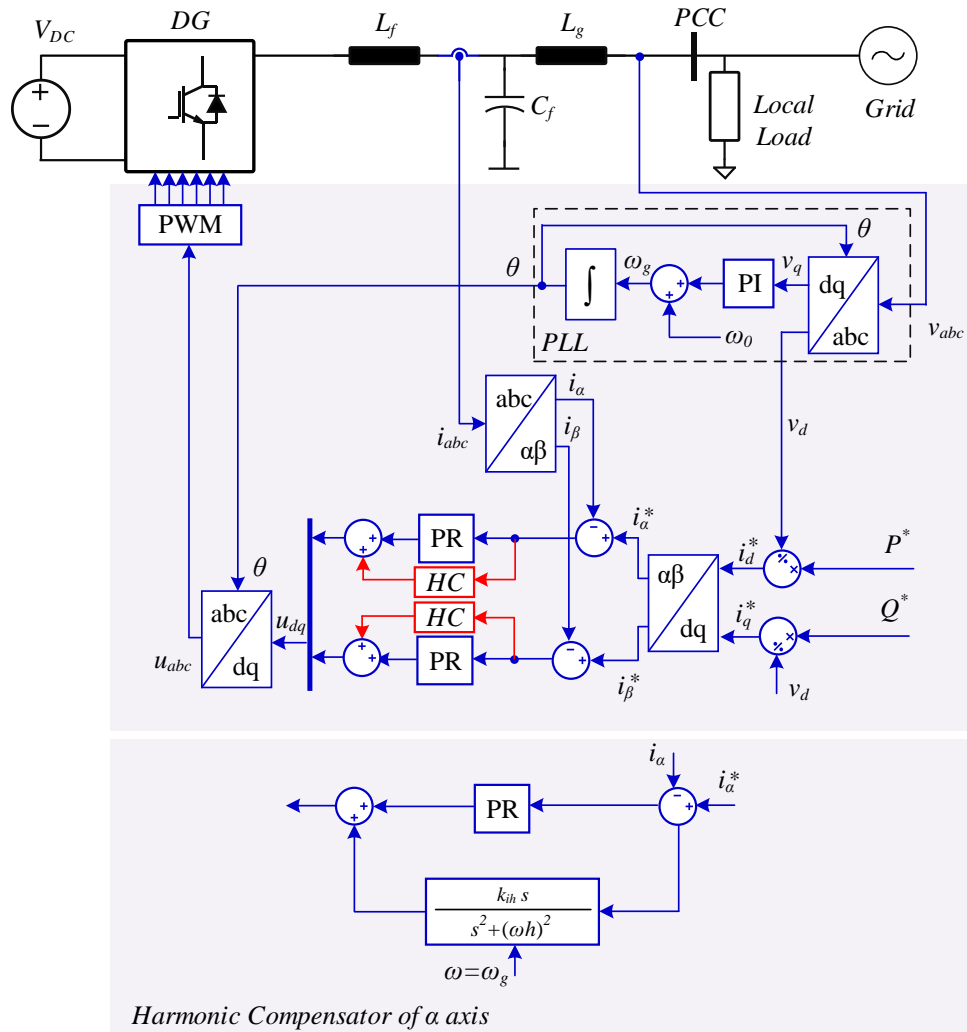


Fig. 28. Basic control structure of a three phase grid following converter generating the reference active  $P^*$  and reactive  $Q^*$  powers with harmonic compensation of the  $h$ -th order harmonic in the  $\alpha\beta$  reference frame.

## 1.4 Grid-synchronization methods– GFM inverters

As discussed in the first section, the synchronization system tasks in converter based DGs, are not only synchronizing the DG to the grid at the start-up point, but also, and more important, keeping the converter to stay synchronized to the grid during the operation by providing the phase angle, frequency, and amplitude of the voltage at the coupling point. In the previous sections, the PLL or improved PLL structures providing the synchronization signals to the control system of the GFL inverters, are discussed in detail as an important part of a control system of DGs. GFLIs typically employ current vector control as their common control method. In contrast, GFMI function as voltage sources and can generate a voltage phasor at their PCC. The inner cascade controller configuration of GFMI is specifically designed to dynamically regulate the angle and magnitude of the voltage phasor at the PCC. This control mechanism ensures synchronization with the grid and provides grid support when required. To achieve this goal, a GFM inverter typically consists of multiple control loops. These loops encompass the current and voltage control loops, virtual impedance loop, active power controller, and reactive power controller. The active power controller is used to control the voltage magnitude, and the reactive power controller is used to control the frequency of the voltage phasor at the PCC. Fig. 29 presents a summary of the control schemes for both active power and reactive power controllers.

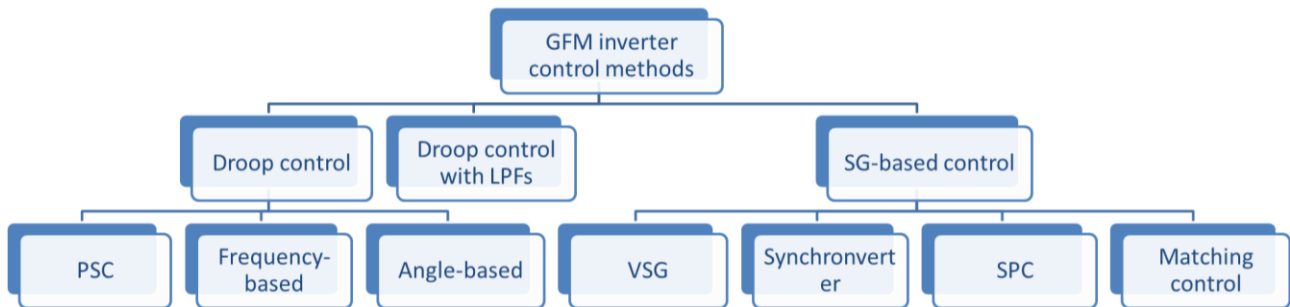


Fig. 29. Control schemes for active power and reactive power controllers

### 1.4.1 Droop control

The droop control mechanism replicates the characteristics of synchronous generators (SGs) in terms of frequency and voltage regulation. It operates by decreasing the frequency when there is an increase in active power and reducing the voltage amplitude when there is an increase in reactive power. The categorization of droop control can be extended by grouping it according to the control law into three main types: frequency-based droop control, angle-based droop control, and power synchronization control (PSC).

#### 1.4.1.1 Frequency-based droop

The frequency-based droop control employs a linear decrease in the inverter's frequency as the power ( $P$ ) increases. This proportional relationship between  $P$  and  $\omega$  is characterized by a droop coefficient  $k_p$ , defining the linear  $P$ -  $\omega$  drooping behavior. The droop coefficient  $k_p$  is configured based on the specific frequency and voltage regulation requirements as outlined in grid codes. Fig. 30 shows the droop control structure. Similarly, the droop-based reactive power control, illustrated in Fig. 30, functions by linearly adjusting the voltage magnitude at the PCC in response to the reactive power injection from the inverter.



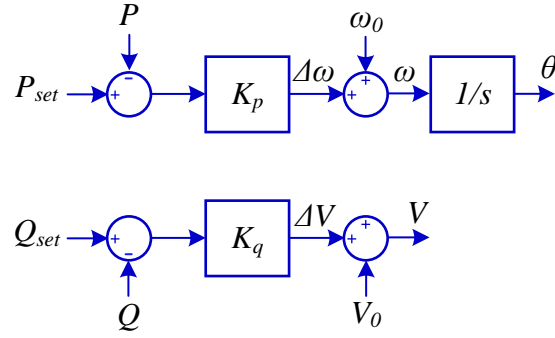


Fig. 30. Control block diagram of basic droop control.

#### 1.4.1.2 Angle-based droop

The angle-based droop control method adopts the power angle ( $\theta$ ) as the control variable, replacing the frequency use. The control utilizes a phase angle relative to a system-wide reference, such as the global positioning system, eliminating the need for inter-inverter communication links. The selection of droop values is determined by the voltage regulation and proportional load sharing prerequisites.

#### 1.4.1.3 Power-synchronization control (PSC)

The Power Synchronization Control (PSC), introduced in (Zhang et al. 2009), is designed to synchronize the voltage source converter with the grid by utilizing a power-synchronization loop known as the active power loop. The control diagram in Fig. 31 illustrates this approach. The active power error is integrated to produce a phase increment denoted as  $\Delta\theta$ , which is combined with the static phase  $\omega_0 t$  to obtain  $\theta$ . From Fig. 31, it becomes evident that the control law utilized in the PSC is identical to that of the frequency-based droop control. This equivalence can also be established through transformations of the control diagram. Initially, the static phase  $\omega_0 t$  can be observed as the integration of  $\omega_0$ . Subsequently, by merging this integrator with the controller's integrator  $k_p/s$ , an equivalent block diagram is derived, showing the mechanism of the frequency-based droop control, as illustrated in Fig. 30.

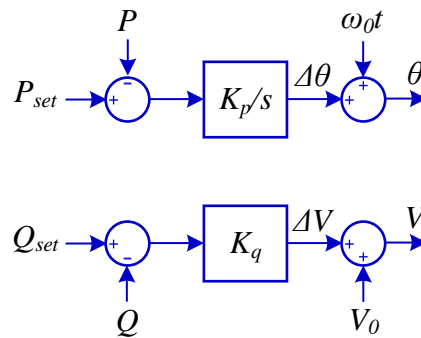


Fig. 31. Control block diagram of a PSC controller.

#### 1.4.2 Droop control with LPFs

In order to mitigate the impact of load imbalances on the measured power components, low pass filters (LPFs) are commonly incorporated into power control loops (Pan et al. 2019), as depicted in Fig. 32. Both the active and reactive power loops employ two LPFs with distinct cutoff frequencies ( $\omega_p, \omega_q$ ). The

implementation of LPFs in the voltage source inverters results in the inadvertent introduction of a virtual inertia effect, comparable to that found in the virtual synchronous generator (VSG).

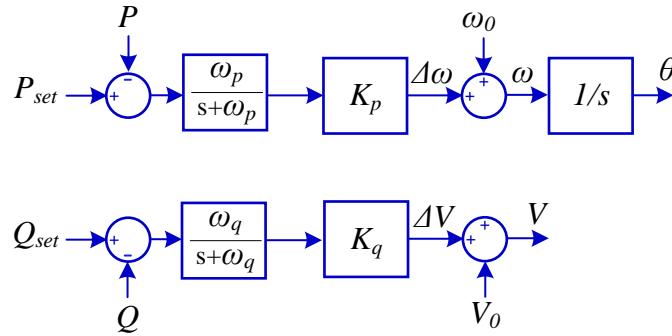


Fig. 32. Control block diagram of droop control with LPFs.

### 1.4.3 SG-based droop control

The droop controller has a significant drawback regarding inertia support. As a result, new control methods are suggested to integrate the inertia and damping characteristics of synchronous generators (SG).

#### 1.4.3.1 VSG control

The VSG technology has been proposed by mimicking the swing equation of an SG. It has been demonstrated in (Pan et al. 2019) that the VSG is equivalent to the droop control for the inertia realization if the active power loop is provided with an LFP. The control diagram of the VSG system is illustrated in Fig. 33. In the VSG, the  $P$ - $\omega$  droop is achieved by modifying the active power reference based on the frequency difference. The droop gain, referred to as the damping factor, is denoted as  $D_p$ . Unlike the PSC and basic droop control, the active power error is not utilized for phase regulation. Instead, it is used for frequency regulation to simulate the inertia  $J$  and mimic the swing equation, which are fundamental properties of the synchronous generator (SG). Similarly, the  $Q$ - $V$  droop is accomplished by adjusting the reactive power reference based on the voltage difference, with  $D_q$  representing the droop gain.

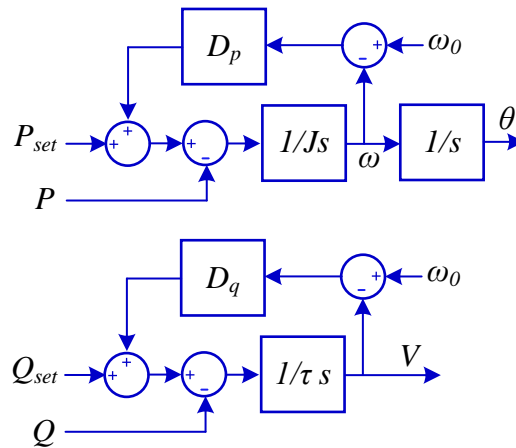


Fig. 33. Control block diagram of a VSG controller.

### 1.4.3.2 SPC control

A VSG control developed for a high inertia condition in the standalone mode could lead to a significant overshoot and an extended settling time in step response in the grid-connected mode. Simultaneously achieving both control objectives defined in the grid-connected and standalone modes is not possible with a VSG control. Hence, in (de Araujo et al. 2022), the VSG control incorporates a zero to develop a lead-lag controller known as SPC. Consequently, the step response is independent of the inertial time constant and droop coefficient. The control diagram of the SPC is depicted in Fig. 34. In contrast to the VSG controller, the SPC offers a supplementary degree of freedom to the system without any increase in the system order, giving a natural  $P - \omega$  droop feature that can be configured independently of the damping and inertia parameters. The transfer function for the SPC is presented below:

$$K_{SPC} = \frac{K_p s + K_i}{s + K_g}$$

The controller gains in the equation, namely  $K_p$ ,  $K_i$ , and  $K_g$ , are used to tune the system's behavior, with  $k_g$  being utilized to configure the system's  $P - \omega$  droop characteristic. Beside, the reactive power control loop utilizes a proportional-integral (PI) controller to adjust the GFM inverter output voltage (de Araujo et al. 2022). Unlike the conventional droop method, the use of an integral controller ensures accurate tracking of zero steady-state reactive power in grid-tied operation. Additionally, when the grid-forming operates in islanding conditions, the integral gain of the PI controller remains fixed at zero.

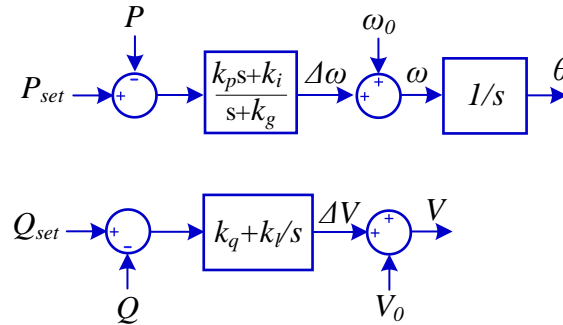


Fig. 34. Control block diagram of an SPC controller.

### 1.4.3.3 Matching control

The authors in (Arghir et al. 2018) have introduced a novel control strategy known as matching control in GFM inverters. This strategy aims to achieve the electromechanical energy transfer of synchronous machines by employing the DC-link voltage. The DC-link voltage serves not only as a pivotal control signal but also as a proxy signal for power imbalances. In (Arghir et al. 2019), the authors propose a comprehensive electronic implementation of the synchronous machine (eSM) and its control design based on energy shaping techniques. Unlike numerical emulation methods, they propose an exact physical realization of the synchronous machine by utilizing the integral of DC bus voltage measurement as the internal angular frequency of the voltage source inverter. This approach allows the representation of physical quantities of synchronous machines, such as the moment of inertia and rotor damping coefficient, using analogous physical quantities of the voltage-source inverter.



discussed. Synchronization for harmonic compensation is also presented which is done in synchronous and stationary reference frames.

Finally, some control algorithms for grid forming inverters are presented including droop control, droop control with low pass filters, and synchronous generators-based control. These control approaches rely on the main principle of the electrical machinery, the synchronous and asynchronous generators. Despite removing the PLL from the control system of these methods, they will be slow because of the virtual inertia emulating the rotating inertia of an electric machine. Hence, this approach is open for research to improve the electric machine-based methods for controlling the converters.

Moreover, utilizing the PLL signals (phase angle, voltage amplitude, and frequency) in the control system of the DGs may affect the stability and resiliency of the system and may make interaction between the DG and the power grid. This can be signified in the case of high penetration of the DGs, like wind turbines in Europe. Therefore, control and synchronization procedure in power electronic based power systems are also open areas for researchers to solve the upcoming issues in this regard.

## References

- Akagi, H., Watanabe, E. & Aredes, M., 2007. *Instantaneous power theory and applications to power conditioning*, John Wiley & Sons.
- Arghir, C., Jouini, T. and Dörfler, F., 2018. Grid-forming control for power converters based on matching of synchronous machines. *Automatica*, 95, pp.273-282.
- Arghir, C. and Dörfler, F., 2019. The electronic realization of synchronous machines: Model matching, angle tracking, and energy shaping techniques. *IEEE Transactions on Power Electronics*, 35(4), pp.4398-4410.
- Ashabani, M. et al., 2016. Inducverters: PLL-Less Converters With Auto-Synchronization and Emulated Inertia Capability. *IEEE Transactions on Smart Grid*, 7(3), pp.1660–1674.
- Benhabib, M.C. & Saadate, S., 2005. A new robust experimentally validated phase locked loop for power electronic control. *EPE journal*, 15(3), pp.36–48.
- Blaabjerg, F. et al., 2006. Overview of Control and Grid Synchronization for Distributed Power Generation Systems. *IEEE Transactions on Industrial Electronics*, 53(5), pp.1398–1409.
- Chapman, S.J., 2005. *Electric Machinery Fundamentals*, Tata McGraw-Hill Education.
- Choi, J.W., Kim, Y.K. & Kim, H.G., 2006. Digital PLL control for single-phase photovoltaic system. In *Proc. IEE Electric Power Applications*. IET, pp. 40–46.
- Ciobotaru, M. et al., 2008. Offset rejection for PLL based synchronization in grid-connected converters. In *Proc. IEEE APEC*. pp. 1611–1617.
- de Araujo Ribeiro, R.L., Oshnoei, A., Anvari-Moghaddam, A. and Blaabjerg, F., 2022. Adaptive Grid Impedance Shaping Approach Applied for Grid-Forming Power Converters. *IEEE Access*, 10, pp.83096-83110.
- Fitzgerald, A. et al., 1990. *Electric Machinery* 6th ed., McGraw-hill.
- Karimi-Ghartemani, M. et al., 2012. Addressing DC Component in PLL and Notch Filter Algorithms. *IEEE Transactions on Power Electronics*, 27(1), pp.78–86.
- Karimi-Ghartemani, M., 2014. *Enhanced phase-locked loop structures for power and energy applications*, John Wiley & Sons.
- Karimi-Ghartemani, M., 2015. Universal Integrated Synchronization and Control for Single-Phase DC/AC Converters. *IEEE Transactions on Power Electronics*, 30(3), pp.1544–1557.
- Karimi-Ghartemani, M. & Iravani, M.R., 2004. A Method for Synchronization of Power Electronic Converters in Polluted and Variable-Frequency Environments. *IEEE Transactions on Power Systems*, 19(3), pp.1263–1270.
- Karimi-Ghartemani, M. & Iravani, M.R., 2001. A new phase-locked loop (PLL) system. In *Proc. IEEE MWSCAS 2001*. pp. 421–424.
- Kundur, P., Balu, N. & Lauby, M., 1994. *Power system stability and control*, New York: McGraw-hill.
- Lasseter, R.H., Chen, Z. and Pattabiraman, D., 2019. Grid-forming inverters: A critical asset for the power grid. *IEEE Journal of Emerging and Selected Topics in Power Electronics*, 8(2), pp.925-935.
- Lin, Y., Eto, J.H., Johnson, B.B., Flicker, J.D., Lasseter, R.H., Villegas Pico, H.N., Seo, G.S., Pierre, B.J. and

- Ellis, A., 2020. Research roadmap on grid-forming inverters (No. NREL/TP-5D00-73476). National Renewable Energy Lab.(NREL), Golden, CO (United States).
- Pan, D., Wang, X., Liu, F. and Shi, R., 2019. Transient stability of voltage-source converters with grid-forming control: A design-oriented study. *IEEE Journal of Emerging and Selected Topics in Power Electronics*, 8(2), pp.1019-1033.
- Rathnayake, D.B., Akrami, M., Phurailatpam, C., Me, S.P., Hadavi, S., Jayasinghe, G., Zabihi, S. and Bahrani, B., 2021. Grid forming inverter modeling, control, and applications. *IEEE Access*, 9, pp.114781-114807.
- Rocabert, J. et al., 2012. Control of power converters in AC microgrids. *IEEE Transactions on Power Electronics*, 27(11), pp.4734–4749.
- Rodríguez, P. et al., 2007. Decoupled Double Synchronous Reference Frame PLL for Power Converters Control. *IEEE Transactions on Power Electronics*, 22(2), pp.584–592.
- Rodríguez, P. et al., 2011. Multiresonant frequency-locked loop for grid synchronization of power converters under distorted grid conditions. *IEEE Transactions on Industrial Electronics*.
- Taul, M.G. et al., 2019. An overview of assessment methods for synchronization stability of grid-connected converters under severe symmetrical grid faults. *IEEE Transactions on Power Electronics*, 34(10), pp.9655-9670.
- Teodorescu, R., Liserre, M. & Rodríguez, P., 2011. *Grid converters for photovoltaic and wind power systems*, John Wiley & Sons.
- Timbus, A.V. et al., 2006. PLL Algorithm for Power Generation Systems Robust to Grid Voltage Faults. In *Proc. IEEE PESC*. pp. 1–7.
- Unruh, P., Nuschke, M., Strauß, P. and Welck, F., 2020. Overview on grid-forming inverter control methods. *Energies*, 13(10), p.2589.
- Valiviita, S., 1999. Zero-crossing detection of distorted line voltages using 1-b measurements. *IEEE Transactions on Industrial Electronics*, 46(5), pp.917–922.
- Woodward Manual, 2004. *Governing Fundamentals and Power Management*. , (Manual 26260).
- Zhang, L., Harnefors, L. and Nee, H.P., 2009. Power-synchronization control of grid-connected voltage-source converters. *IEEE Transactions on Power systems*, 25(2), pp.809-820.
- Zhong, Q. & Weiss, G., 2011. Synchronverters: Inverters That Mimic Synchronous Generators. *IEEE Transactions on Industrial Electronics*, 58(4), pp.1259–1267.